Heavy Fermions and Quantum Phase Transitions

Qimiao Si[1]* and Frank Steglich[2]*

Quantum phase transitions arise in many-body systems because of competing interactions that promote rivaling ground states. Recent years have seen the identification of continuous quantum phase transitions, or quantum critical points, in a host of antiferromagnetic heavy-fermion compounds. Studies of the interplay between the various effects have revealed new classes of quantum critical points and are uncovering a plethora of new quantum phases. At the same time, quantum criticality has provided fresh insights into the electronic, magnetic, and superconducting properties of the heavy-fermion metals. We review these developments, discuss the open issues, and outline some directions for future research.

Quantum mechanics not only governs the subatomic world but also dictates the organization of the microscopic particles in bulk matter at low temperatures. The behavior is strikingly different depending on the spin (the internal angular momentum) of the constituent particles. Particles whose spin is an integer multiple of $\hbar$ (Planck's constant h divided by 2π) are bosons. When cooled down to sufficiently low temperatures, they will be described by the same wave function, forming a "condensate." Particles whose spin is a half-integer of $\hbar$, on the other hand, are fermions satisfying the Pauli exclusion principle; no two particles can have the same state. At absolute zero, they occupy the states with the lowest energies, up to an energy referred to as the Fermi energy. In the momentum space, this defines a Fermi surface, enclosing a Fermi volume in which all the states are occupied.

When the particle-particle interactions are included, the behavior of such quantum systems becomes even richer. These strongly correlated systems have taken the center stage in the field of quantum matter over the past two decades (*1*). High-temperature superconductors, fractional quantum Hall systems, colossal magnetoresistive materials, and magnetic heavy-fermion metals are a few prominent examples. The central question for all these systems is how the electrons are organized and, in particular, whether there are principles that are universal among the various classes of these strongly correlated materials. One such principle, which has come to the forefront in recent years, is quantum criticality (*2*).

A quantum critical point (QCP) arises when matter undergoes a continuous transition from one phase to another at zero temperature. A nonthermal control parameter, such as pressure, tunes the amount of zero-point motion of the constituent particles. In other words, such a parameter controls quantum-mechanical tunneling dictated by Heisenberg's uncertainty principle, changing the degree of quantum fluctuations. This is the analog of varying the thermal fluctuations in the case of temperature-driven classical phase transitions, such as the melting of ice or the loss of ferromagnetic order in iron.

The temperature-pressure phase diagram observed in the heavy-fermion intermetallic compound $CePd_2Si_2$ is illustrated in Fig. 1A (*3*). At ambient pressure, $CePd_2Si_2$ orders into an antiferromagnet, below the Néel temperature T_N of about 10 K. Applying pressure reduces T_N monotonically, eventually suppressing the antiferromagnetic order altogether and turning the system into a paramagnetic metal. The putative critical pressure p_c is around 2.8 GPa, at which point an antiferromagnetic QCP is implicated. The QCP, however, is not explicitly observed. Instead, a "dome" emerges at very low temperatures in the vicinity of p_c, under which the system is a superconductor.

This phase diagram exemplifies a general point. It suggests that antiferromagnetic quantum criticality can provide a mechanism for superconductivity—an observation that may be of relevance to a range of other strongly correlated systems, such as high–critical temperature (T_c) cuprates, organic superconductors, and the recently discovered high-T_c iron pnictides. The formation of new phases near a QCP may be considered the consequence of an accumulation of entropy, which is a generic feature of any QCP (*4*) and has recently been observed experimentally (*4*–*6*).

A good example for such an antiferromagnetic QCP is the one observed in the compound $YbRh_2Si_2$ (*4*). Here, the nonthermal control parameter is a (small) magnetic field. The studies of heavy-fermion antiferromagnets have shown that accompanying the QCP at zero temperature is a finite parameter range at nonzero temperatures, in which the metallic state is anomalous (Fig. 1B) (*7*, *8*). Over this quantum critical regime, the electrical resistivity is linear in temperature—a telltale sign for an unusual metallic state. This non-Fermi liquid behavior (*9*), which goes beyond the standard theory of metals [Fermi-liquid theory (*10*)], is another phenomenon that is broadly relevant to the physics of strongly correlated systems (*11*, *12*).

Quantum criticality has been implicated to one degree or another in a host of other heavy-fermion metals (*4*, *13*, *14*). These include $CeCu_2Si_2$, the first superconductor to be observed among heavy-fermion metals (*15*), and $CeRhIn_5$ (Fig. 1C) (*16*). Extensive theoretical studies have led to unconventional quantum criticality (*17*–*20*). More recently, a plethora of phases have been uncovered in heavy-fermion metals near a QCP [such as in Ir-doped $YbRh_2Si_2$ (*8*) and in β-$YbAlB_4$ (*21*)]. Together with the theoretical studies of the global phase diagram of the heavy-fermion metals (*22*, *2*), these developments open up an entirely new frontier on the interplay between quantum criticality and unusual phases.

Quantum Phase Transitions

Quantum phase transitions result from the variation of quantum fluctuations. Tuning a control parameter at absolute zero temperature tilts the balance among the competing ground states associated with conflicting interactions of quantum matter.

Heavy-fermion metals comprise a lattice of localized magnetic moments and a band of conduction electrons (*10*). The exchange interaction between the local moments is primarily that mediated by the conduction electrons: the familiar Ruderman-Kittel-Kasuya-Yoshida (RKKY) interaction. This interaction drives the local moments into an ordered pattern, much like H_2O molecules are condensed into an ordered arrangement in ice. The Kondo-exchange interaction between the local moments and conduction electrons introduces spin flips, which is a tunneling process enabled by quantum mechanics. Correspondingly, increasing the Kondo interaction amounts to enhancing quantum fluctuations, which eventually destroys the magnetic order and yields a paramagnetic phase (*23*, *24*).

The theory of classical phase transitions, formulated by Landau (*25*), is based on the principle of spontaneous symmetry breaking. Consider $CePd_2Si_2$ at ambient pressure. In the paramagnetic phase, at $T > T_N$, the spins are free to rotate. Upon entering the magnetically ordered phase, this continuous spin-rotational symmetry is spontaneously broken; the spins must choose preferred orientations. In the Landau formulation, this symmetry distinction is characterized by a quantity called order parameter; in our case, this is the staggered magnetization of the antiferromagnet. The order parameter is nonzero in the magnetically ordered phase but vanishes in the paramagnetic phase. The critical point arises when the phase transition is continuous—when the order parameter goes to zero smoothly. It is described in terms of the spatial fluctuations of the order parameter. These fluctuations occur over a char-

[1]Department of Physics and Astronomy, Rice University, Houston, TX 77005, USA. [2]Max Planck Institute for Chemical Physics of Solids, 01187 Dresden, Germany.

*To whom correspondence should be addressed. E-mail: qmsi@rice.edu (Q.S.); steglich@cpfs.mpg.de (F.S.)

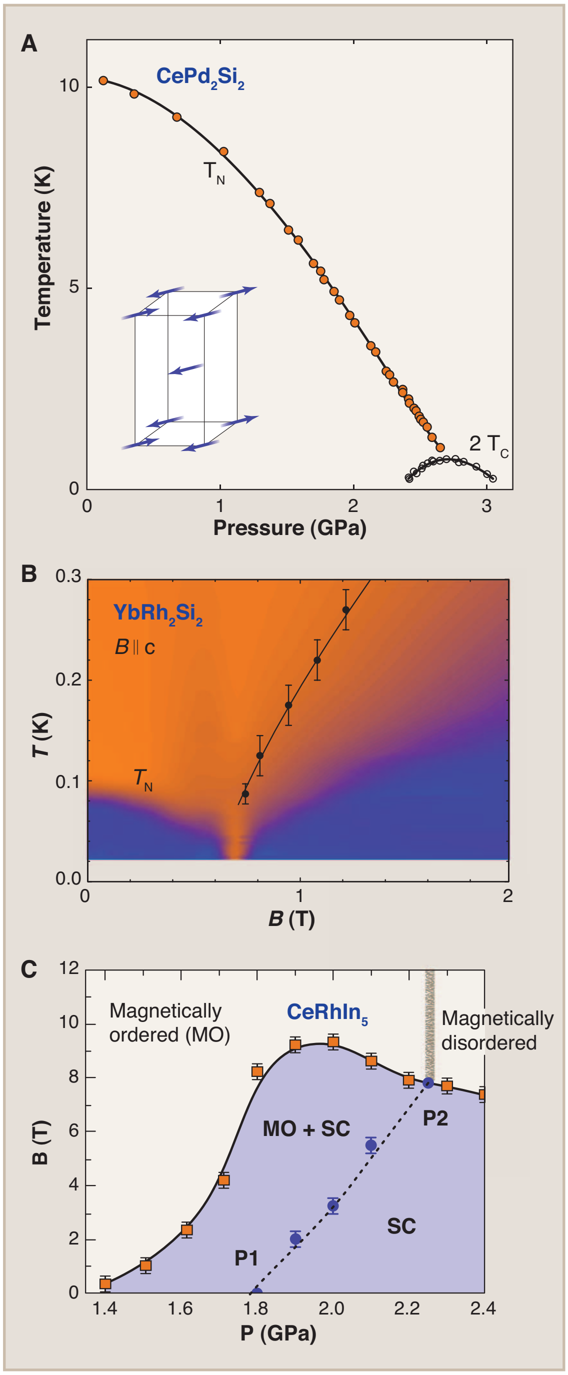

Fig. 1. Quantum phase transitions in heavy-fermion metals. (**A**) Suppression of antiferromagnetic order through pressure in $CePd_2Si_2$. T_N is the Néel transition temperature, and the corresponding antiferromagnetic order is illustrated in the inset. At the boundary of the antiferromagnetism, a phase of unconventional superconductivity arises. T_c corresponds to the superconducting transition temperature (*3*). (**B**) Field-induced quantum phase transition in $YbRh_2Si_2$. The blue regions label the Fermi-liquid behavior observed with measurements of electrical resistivity and other transport and thermodynamic properties; they correspond to $T < T_N$ at $B < B_N$ and $T < T_{FL}$ at $B > B_N$, where B_N is the critical field at $T = 0$. The orange region describes non-Fermi liquid behavior that is anchored by the QCP at $B = B_N$ (*7*). The (T^*) line delineates crossover behavior associated with the destruction of the Kondo effect (*8*). (**C**) The pressure-field phase diagram at the lowest measured temperature ($T = 0.5$ K) in $CeRhIn_5$. The antiferromagnetic order, denoted by MO, at ambient pressure gives way to superconductivity, specified by SC, at higher pressures. At $B = 0$, the antiferromagnetic order goes away when the pressure exceeds P_1. When the magnetic field exceeds just enough to suppress superconductivity, the system is antiferromagnetically ordered at lower pressures ($P < P_2$) but yields a nonmagnetic phase at higher pressures ($P > P_2$). The hatched line refers to the transition at P_2, between these two phases (*37*).

acteristic length scale, which increases on approaching the critical point. At the critical point, the correlation length is infinite. Correspondingly, physical properties are invariant under a mathematical operation that dilates the lengths; in other words, they are scale-invariant.

A straightforward generalization of the Landau paradigm to QCPs gives rise to essentially the same theoretical description (*26*). Quantum mechanics introduces a "time" axis: Quantum states evolve in time. (For quantum systems in equilibrium, the relevant quantum evolution is along an imaginary time of length $\hbar/k_BT$, where k_B is the Boltzmann constant.) This introduces a time scale that accompanies the divergent correlation-length scale. When the transition takes place at a finite temperature T_N, $\hbar/k_BT_N$ serves as the upper bound of the correlation time, and the ultimate critical behavior is still determined by the fluctuations in space only. When T_N is driven to zero temperature, however, a divergent correlation time ξ_τ accompanies the divergent correlation length ξ, and both must be taken into account even for equilibrium properties. Hence, the quantum critical fluctuations of the order parameter take place both in space and in time. The effective dimensionality of the fluctuations is $d + z$, where d is the spatial dimensionality, and z, the dynamic exponent defined in terms of the relationship $\xi_\tau \propto \xi^z$, describes the number of effective spatial dimensions to which the time dimension corresponds.

However, it has been appreciated that this Landau paradigm can break down for QCPs. Consider the effect of the Kondo-exchange coupling. In addition to destabilizing the magnetic order, the Kondo interaction also introduces quantum coherence between the local moments and conduction electrons. Indeed, inside the paramagnetic phase a process called Kondo screening takes place, which leads to a qualitatively new ground state in which the local moments and conduction electrons are entangled. Just as a continuous onset of magnetic order at zero temperature introduces quantum fluctuations of the magnetic order parameter, a critical onset of Kondo entanglement also yields its own quantum critical degrees of freedom. When that happens, a new type of QCP ensues.

Kondo Effect and Heavy Fermions

Historically, the Kondo screening effect was introduced for dilute magnetic impurities in metallic hosts (*10*). By the 1970s, the notion that the Kondo phenomenon operates in a dense periodic array of magnetic Ce ions in intermetallic compounds, such as $CeAl_2$ (*27*), was already in place. A characteristic scale, at which the Kondo screening initially sets in, is the Kondo temperature T_K.

The list of heavy-fermion materials is long, and they are typically compounds containing rare earths or actinides (including Yb, U, and Np, in addition to Ce) with partially filled 4f- or 5f-orbitals. Their defining characteristic is that the effective mass of the charge carriers at the lowest accessible temperatures is hundreds of times the bare electron mass.

Microscopically, heavy-fermion systems can be modeled as a lattice of localized f-electron moments that are coupled to a band of conduction electrons. In the early 1980s, the description of the Kondo effect in the ground state of this Kondo lattice was formulated (*10*). The local moments lose their identity by forming a many-body spin singlet with all the conduction electrons, leading to an entangled state (Fig. 2A). The Kondo entanglement in the ground state makes the local moments, which are charge-neutral to begin with, acquire the quantum numbers of the conduction electrons, namely spin-$\hbar/2$ and charge-e. Correspondingly, "Kondo resonances" appear as charge carriers, and they remember their localized-moment origin by possessing a heavy mass. Because the Kondo resonances are part of the electronic-excitation spectrum, they must be accounted for in the Fermi surface, leading to the notion of a large Fermi surface (Fig. 2B)—the picture of a heavy Fermi liquid.

The Kondo resonances can alternatively be thought of as the remnants of the original f-electrons. They are delocalized because the 4f- or 5f-wave function has a finite overlap with the ligand orbitals that form the conduction electrons. In other words, the f-electrons and conduction electrons are hybridized.

QCPs in Heavy Fermions

Two types of QCPs. The Kondo singlet in the ground state of a heavy-fermion paramagnet represents an organized macroscopic pattern of the quantum many-body system (Fig. 2A). It endows the paramagnetic phase at zero temperature with a quantum order. This characterization of the phase goes beyond the Landau framework. The Kondo-singlet state does not invoke any spontaneous breaking of symmetry because the spins can orient in arbitrary directions; no Landau order parameter can be associated to the Kondo effect. Two types of QCPs arise, depending on the behavior of the Kondo singlet as we approach the QCP from the paramagnetic side.

When the Kondo singlet is still intact across the antiferromagnetic transition at zero temperature, the only critical degrees of freedom are the fluctuations of the magnetic order parameter. In this case, the antiferromagnetically ordered phase in the immediate proximity to the QCP can be described in terms of a spin-density-wave (SDW) order of the heavy quasiparticles of the paramagnetic phase. The QCP is referred to as of the SDW type, which is in the same class as that already considered by Hertz (*26*, *28*–*30*). On the other hand, when the Kondo singlet exists only in the paramagnetic phase, the onset of magnetic order is accompanied by a breakdown of the Kondo effect. The quantum criticality incorporates not only the slow fluctuations of the antiferromagnetic order parameter but also the emergent degrees of freedom associated with the breakup of the Kondo singlet. The corresponding transition is referred to as locally critical (*17*, *18*); the antiferromagnetic transition is accompanied by a localization of the f-electrons.

This distinction of the two types of QCPs can also be made in terms of energetics. The key quantity to consider is the energy scale E^*, which dictates the breakup of the entangled Kondo singlet state as the system moves from the heavy-Fermi-liquid side toward the quantum critical regime. A reduction of the E^* scale upon approaching the magnetic side is to be expected because the development of antiferromagnetic correlations among the local moments reduces the strength of the Kondo singlet (*17*–*20*). When E^* remains finite at the antiferromagnetic QCP, the Kondo singlet is still formed, and the quantum criticality falls in the universality class of the SDW type. When the E^* scale continuously goes to zero at the antiferromagnetic QCP, a critical Kondo breakdown accompanies the magnetic transition. The T_K scale, in which the Kondo screening initially sets in, is always nonzero near the QCP, even when E^* approaches zero.

The consequence of the Kondo breakdown for the change of the Fermi surface is illustrated in Fig. 2. When E^* is finite, the Kondo-singlet ground state supports Kondo resonances, and the Fermi surface is large. When the E^* scale becomes zero, the ground state is no longer a Kondo singlet, and there are no fully developed Kondo resonances. Correspondingly, the Fermi surface is small, incorporating only the conduction electrons.

In the Kondo-screened paramagnetic phase (Fig. 2A), the large Fermi surface is where the heavy quasiparticles are located in the momentum space (Fig. 2B). As usual, such sharply defined Fermi surfaces occur below an effective Fermi temperature, T_{FL}. Below this temperature, standard Fermi-liquid properties—such as the inverse quasiparticle lifetime and the electrical resistivity being quadratically dependent on temperature—take place.

In the Kondo-destroyed antiferromagnetic phase (Fig. 2C), there is no Kondo singlet in the ground state, and correspondingly, static Kondo screening is absent. Kondo screening still operates dynamically, leading to an enhancement of the mass of the quasiparticles. The quasiparticles still have a Fermi-liquid form at low temperatures. In contrast to the case of the Kondo-singlet ground state, these quasiparticles are adiabatically connected to the ordinary conduction electrons and are located at the small Fermi surface (Fig. 2D).

The large number of available compounds is a key advantage in the study of quantum critical heavy-fermion systems. At the same time, it raises an important question: Can we classify the quantum critical behavior observed in these heavy-fermion compounds? Below, we summarize the evidence for such a classification in the systems that have been most extensively studied in the present context.

QCP of the SDW type. The phase diagram for $CePd_2Si_2$ (Fig. 1A) (*3*) is reminiscent of theoretical discussions of unconventional superconductivity near an SDW instability. Unfortunately, because of the high pressure necessary to access the QCP in this compound, it has not yet been possible to study either the order or the fluctuation spectrum near the QCP. $CeCu_2Si_2$ is an ideal system for such an investigation because, here, heavy-fermion superconductivity forms in the vicinity of an antiferromagnetic QCP at ambient/low pressure. Neutron diffractometry revealed the antiferromagnetically ordered state to be an incommensurate SDW with small ordered moment (~0.1 μ_B/Ce) because of the nesting of the renormalized Fermi surface (*31*). Inelastic neutron-scattering studies on paramagnetic $CeCu_2Si_2$ have identified fluctuations close to the incommensurate ordering wave vector of the nearby SDW and have shown that such fluctuations play a dominant role in driving superconducting pairing (*32*), confirming earlier theoretical predictions.

Another compound is $CeNi_2Ge_2$, for which the magnetic instability may be achieved by slight volume expansion. The critical Grüneisen ratio in this system diverges as T^{-1}, which lends support for a nearby SDW QCP (*4*).

There are also a few examples of magnetic quantum phase transitions induced by alloying that appear to fall in the category of the SDW QCP. In $Ce_{1-x}La_xRu_2Si_2$, for instance, recent inelastic neutron-scattering experiments have provided such evidence near its critical concentration $x_c \approx 0.075$ (*33*).

QCP involving a Kondo breakdown. As shown in Fig. 3A, inelastic neutron-scattering

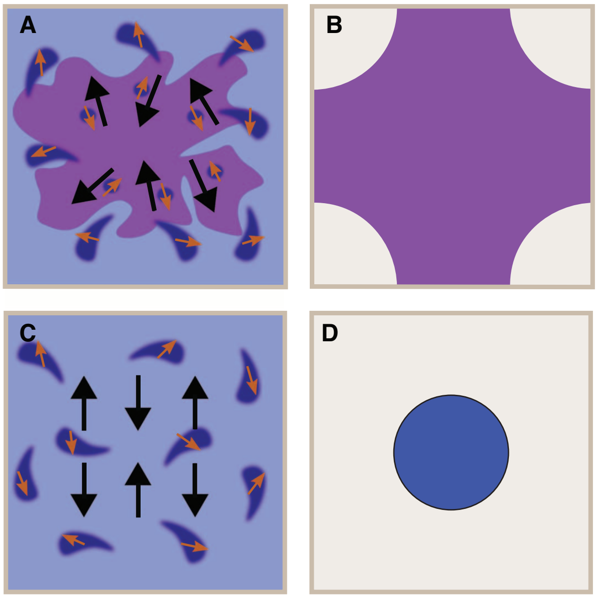

Fig. 2. Kondo entanglement and its breakdown in heavy-fermion metals. (**A**) Kondo-singlet ground state in a paramagnetic phase, giving rise to a heavy Fermi liquid. The shapes with orange arrows indicate the mobile conduction electrons, and the thick black arrows indicate localized magnetic moments. The purple profile describes the Kondo singlet in the ground state. (**B**) The Kondo singlet in the ground state gives rise to Kondo resonances, which must be incorporated into the Fermi volume. Correspondingly, the Fermi surface is large, with a volume that is proportional to $1 + x$, where 1 and x, respectively, refer to the number of local moments and conduction electrons per unit cell. An SDW refers to an antiferromagnetic order that develops from a Fermi-surface instability of these quasiparticles. (**C**) Kondo breakdown in an antiferromagnetic phase. The local moments arrange into an antiferromagnetic order among themselves, and they do not form static Kondo singlets with the conduction electrons. (**D**) Kondo resonances do not form in the absence of static Kondo screening. Correspondingly, the Fermi surface is small, enclosing a volume in the paramagnetic Brillouin zone that is proportional to x. Dynamical Kondo screening, however, still operates, giving rise to an enhancement of the quasiparticle mass near the small Fermi surface.

experiments on the quantum critical material $CeCu_{5.9}Au_{0.1}$ revealed an energy over temperature (E/T) scaling (*34*) of the dynamical susceptibility, with a fractional exponent (*35*). The same critical exponent is found to govern the magnetic susceptibility at wave vectors far away from the antiferromagnetic wave vector. These features are incompatible with the predictions of the SDW theory (*26*, *28*–*30*) and have provided the initial motivation for the development of local quantum criticality (*17*). Because such a QCP involves a breakdown of the Kondo effect, it must be manifested in the charge carriers and their Fermi surfaces as well.

Direct measurements of Fermi surfaces are typically done by using angle-resolved photoemission spectroscopy (ARPES). In spite of impressive recent developments, ARPES still does not have the resolution to study heavy-fermion metals in the required sub-Kelvin low-temperature range. The other well-established means to probe Fermi surfaces is the de Haas–van Alphen (dHvA) technique, which, however, requires a large magnetic field of several teslas. A rare opportunity arises in $CeRhIn_5$, in which a magnetic field of about 10 T is in fact needed to suppress superconductivity and expose a quantum phase transition (Fig. 1C). From dHvA measurements performed in the field range of 10 to 17 T, a pronounced jump in the Fermi surface was seen in $CeRhIn_5$ at the critical pressure of 2.3 GPa (Fig. 3B) (*36*). This, together with the observation of a seemingly diverging cyclotron mass of the heavy charge carriers, is commonly considered as evidence for a Kondo-breakdown QCP (*37*). We caution that for $CeRhIn_5$, this issue remains to be fully settled; an alternative explanation that is based on a change of the valence state of the Ce ions has also been made (*38*).

The heavy-fermion metal $YbRh_2Si_2$ has provided an opportunity to probe the electronic properties near an antiferromagnetic QCP involving a breakdown of the Kondo effect. As mentioned earlier, the very weak antiferromagnetic order of $YbRh_2Si_2$ is suppressed by a small magnetic field, giving way to non-Fermi liquid behavior (*7*). Furthermore, the magnetic field induces a substantial change of the isothermal Hall coefficient. The latter has been shown to probe, at low temperatures, the properties of the Fermi surface (*39*). A new temperature scale, $T^*(B)$, was identified in the T–B phase diagram of $YbRh_2Si_2$ (Fig. 1B); across this scale, the isothermal Hall coefficient exhibits a crossover as a function of the applied magnetic field (B). This crossover sharpens upon cooling. Extrapolation to $T = 0$ suggests an abrupt change of the Fermi surface at the critical magnetic field B_N, the field where T_N approaches zero (*39*). Further evidence for the inferred change of Fermi surface has come from thermotransport measurements (*40*). Across the T^* line, the low-temperature thermopower shows a sign change, suggesting an evolution between hole-like and electron-like Fermi surfaces, as illustrated in Fig. 2, B and D.

Further thermodynamic and transport investigations confirmed $T^*(B)$ to be an intrinsic energy scale that vanishes at the antiferromangetic QCP (Fig. 4A) (*41*). The T^* scale is distinct from the Fermi-liquid scale T_{FL}, below which a T^2 resistivity is observed (Fig. 4A). These properties are naturally interpreted as signatures of a breakdown of the Kondo effect at the QCP, with the Fermi surface being large at $B > B_N$ (Fig. 2, A and B) and being small at $B < B_N$ (Fig. 2, C and D); T^* refers then to the temperature scale accompanying the Kondo-breakdown energy scale E^* introduced earlier. Notably, the E^* scale is distinct from the aforementioned T_K scale, which serves as the upper cut-off of the quantum-critical scaling regime and should therefore remain finite near the QCP. For instance, at the critical concentration of $CeCu_{6-x}Au_x$ T_K has been observed in photoemission spectroscopy to be nonzero (*42*), even though E^* is expected to vanish.

A recent thorough study of the Hall crossover on $YbRh_2Si_2$ single crystals of substantially improved quality showed unequivocally that the width of the crossover at $T^*(B)$ is strictly proportional to temperature (Fig. 4B) (*43*). This indicates that the E/T scaling also operates in this compound. Furthermore, it provides evidence that the Kondo-breakdown effect indeed underlies such quantum critical scaling (*43*).

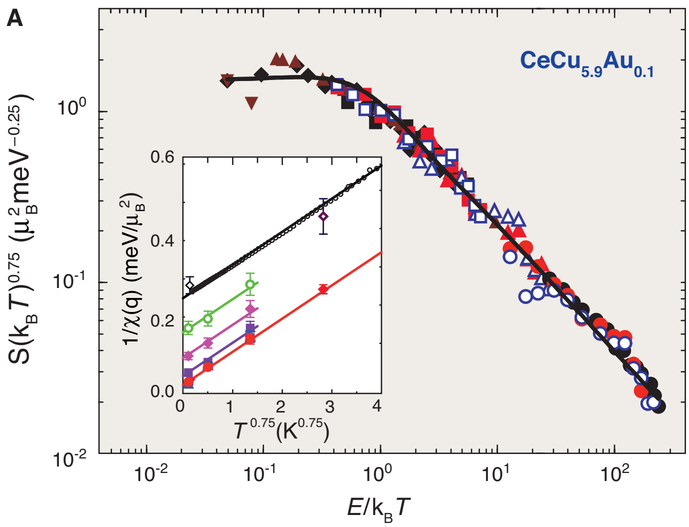

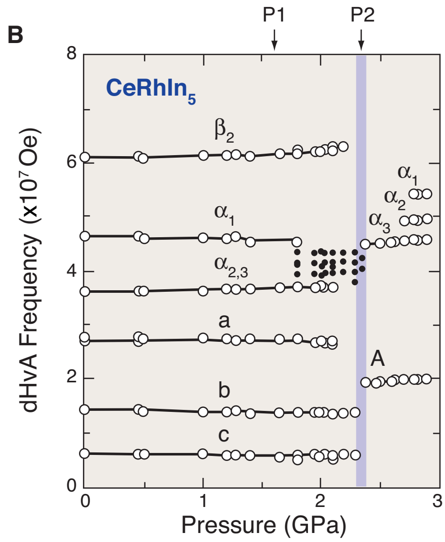

Fig. 3. Quantum critical properties of $CeCu_{6-x}Au_x$ and $CeRhIn_5$. (**A**) Quantum-dynamical E/T scaling of the inelastic neutron-scattering cross-section S in $CeCu_{5.9}Au_{0.1}$. The measurements were performed at the antiferromagnetic wave vectors (where S is maximized), and the scaling collapse is constructed in the form of $T^{\alpha}S$ as a function of E/T. The temperature and energy exponent is fractional: $\alpha = 0.75$. The different symbols represent data taken in different spectrometers at the different peak wave vectors. (Inset) The inverse of the bulk magnetic susceptibility, $1/\chi(\mathbf{q} = 0) \equiv H/M$, and that of the static susceptibility at other wave vectors derived from the dynamical spin susceptibility through the Kramers-Kronig relation (*35*). (**B**) Several dHvA frequencies as a function of pressure in $CeRhIn_5$. The applied magnetic field ranges between 10 T and 17 T. P_1 and P_2 have the same meaning as in Fig. 1C. The symbols denote different branches of the Fermi surface (*36*).

Global Phase Diagram

The fact that in $YbRh_2Si_2$, the multiple lines defining the Kondo-breakdown scale T^*, the Fermi-liquid scale T_{FL}, and the Néel-temperature scale T_N all converge at the same magnetic field in the zero-temperature limit raises the question of what happens when some additional control parameter is varied. This global phase diagram has recently been explored by introducing chemical pressure to $YbRh_2Si_2$ (*8*). The antiferromagnetic order is stabilized or weakened by means of volume compression or expansion, respectively (Fig. 4, C to E), in accordance with the well-established fact that pressure reinforces magnetism in Yb-based intermetallics. Unexpectedly however, the $T^*(B)$ line is only weakly dependent on chemical pressure. Under volume compression (3% Co-doping), the antiferromagnetic QCP occurs at a field substantially higher than B^*, at which $T^* \to 0$ (Fig. 4E). In this situation, T^* is finite at the antiferromagnetic QCP. One therefore expects that the SDW description will apply, and this is indeed observed (*8*). Under a small volume expansion (2.5% Ir-doping), B_N and B^* continue to coincide within the experimental accuracy (Fig. 4D). With a large volume expansion (17% Ir-doping), on the other hand, B_N has vanished, but B^* remains finite (Fig. 4C). This opens up a range of magnetic field in which not only any magnetic ordering is absent but also the Kondo-breakdown scale vanishes, suggesting a small Fermi surface. Hydrostatic-pressure experiments (*44*) on undoped $YbRh_2Si_2$ give results comparable with those of the Co-doped materials with a similar average unit-cell volume, indicating that the crossing of $T_N(B)$ and $T^*(B)$ as observed (*8*) for 7% Co-doped $YbRh_2Si_2$ originates from the alloying-induced volume compression rather than disorder.

The results can be summarized in the global phase diagram shown in Fig. 4F. The transition from the small-Fermi-surface antiferromagnet to the heavy-Fermi-liquid state has three types. It may go through a large-Fermi-surface antiferromagnet, such as in the Co-doped cases. The transition can also occur directly, such as in the pure and 2.5% Ir-doped compounds. Or, it may go through a small-Fermi-surface paramagnetic phase, such as in the case of the 6% Ir-doped $YbRh_2Si_2$ (*8*). In this phase, the electrical resistivity shows a quasi-linear temperature dependence (*8*).

Theoretically, two kinds of antiferromagnet–to–heavy-Fermi-liquid transitions were already considered in the previous section. One way to connect them is to invoke a $T = 0$ global phase diagram (*22*), spanned by two parameters associated with two types of quantum fluctuations. One parameter, J_K, describes the Kondo coupling between the conduction electrons and the local moments; increasing J_K enhances the ability of the conduction electrons to screen the local moments and reduces the magnetic order. The other parameter, G, is associated with the interactions among the local moments and refers to, for instance, the degree of geometric frustration (*45*) or simply the dimensionality (*17*, *46*); raising the parameter G boosts the inherent quantum fluctuations of the local-moment system and correspondingly weakens the magnetism. In the two-parameter global phase diagram of (*22*), each kind of transition appears as a line of critical points: One line is associated with local quantum criticality, with the breakdown of the Kondo effect occurring at the antiferromagnetic-ordering transition; the other one is associated with SDW quantum criticality, in which case the Kondo breakdown can only take place inside the antiferromagnetically ordered region. This is consistent with Fig. 4F, in which B_N and B^* coincide for a finite range of small Ir concentrations. The extension of this global phase diagram is currently being pursued theoretically (*2*). When the quantum fluctuations among the local moments are even stronger, a possibility exists for a paramagnetic phase with a suppressed Kondo entanglement and a concomitant small Fermi surface; this can be compared with the region highlighted by the question marks in Fig. 4F. This phase could be a spin liquid or could be an ordered state (such as a spin-Peierls phase) that preserves the spin-rotational invariance. Understanding the nature of the phase represents an intriguing problem worthy of further study, both theoretically and experimentally.

Other heavy-fermion systems may also be discussed in this two-parameter global phase diagram. The zero-temperature transition in $CeCu_{6-x}Au_x$ as a function of doping or pressure can be described in terms of local quantum criticality. As a function of magnetic field, for both $CeCu_{6-x}Au_x$ (*47*) and $CeIn_3$ (*48*) the Kondo breakdown seems to take place inside the antiferromagnetic part of the phase diagram. It will be instructive to see whether other heavy-fermion materials can be used to map the global phase diagram and, in particular, display a paramagnetic non-Fermi liquid phase near a Kondo-breakdown QCP.

Conclusions and Outlook

Studies in the last decade have firmly established the existence of QCPs in heavy-fermion metals. These transitions arise from the suppression of long-range antiferromagnetic ordering by means of tuning pressure, chemical composition, or magnetic field. An important property of QCPs is the accumulation of entropy. Correspondingly, the Grüneisen ratio or the magnetocaloric effect diverges, which serves as an important thermodynamic characterization of the QCPs.

Two types of QCPs have been developed for antiferromagnetic heavy-fermion systems. When a breakdown of the Kondo entanglement occurs inside the antiferromagnetically ordered phase, the QCP has the standard SDW form that conforms to Landau's paradigm of order-parameter fluctuations. When such a Kondo breakdown

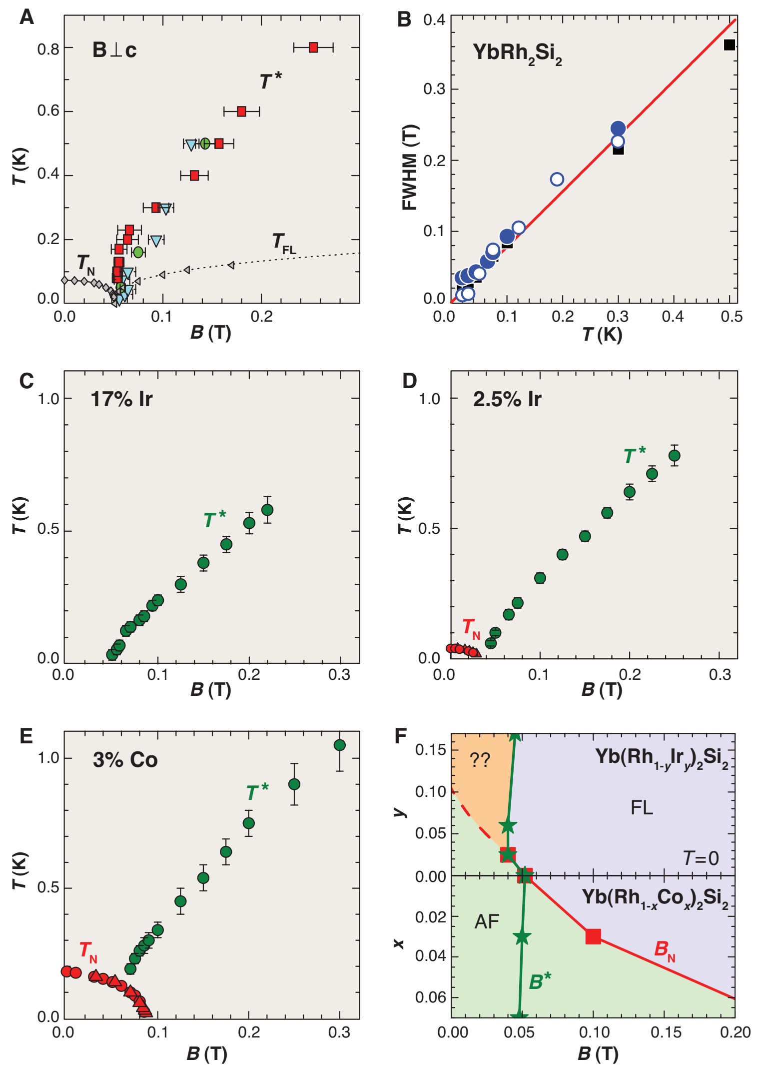

Fig. 4. Quantum criticality and global phase diagram in pure and doped $YbRh_2Si_2$. (**A**) Multiple energy scales in pure $YbRh_2Si_2$. T^* is extracted from isothermal crossovers in the Hall effect and thermodynamic properties, which is interpreted in terms of a Kondo breakdown. T_{FL} is the scale below which Fermi-liquid properties occur. Both crossover lines merge with the line that specifies the magnetic phase boundary T_N in the zero-temperature limit, at B_N (*41*). (**B**) Full width at half maximum (FWHM) of the crossover in the Hall coefficient of a high-quality single crystal (*RRR* = 120). It extrapolates to zero in the $T = 0$ limit, implying a jump of the Hall coefficient and other properties. It is proportional to temperature, suggesting a quantum-dynamical E/T scaling (*43*). (**C** to **E**) $T^*(B)$ and $T_N(B)$ lines for Ir- and Co-doped $YbRh_2Si_2$, determined via AC susceptibility measurements (*8*). Data for the 7% Co-doped $YbRh_2Si_2$ show an intersection of the two lines (*8*). (**F**) The $T = 0$ phase diagram, doping-concentration versus magnetic field, for $Yb(Rh_{1-x}M_x)_2Si_2$, M=Co,Ir (*8*).

happens at the onset of antiferromagnetism, a new class of QCP arises. Evidence for this local quantum criticality has come from the quantum-dynamical scaling and mass divergence in $CeCu_{6-x}Au_x$ and $YbRh_2Si_2$, the multiple energy scales observed in $YbRh_2Si_2$, and the jump of the Fermi surface in $YbRh_2Si_2$ and $CeRhIn_5$.

A strong case has been made that in $CeCu_2Si_2$, the critical fluctuations of a SDW QCP promote unconventional superconductivity. It is likely that the superconductivity in $CePd_2Si_2$ has a similar origin. Whether the Kondo-breakdown local QCPs also favor superconductivity is less clear. $CeRhIn_5$ under pressure and β-$YbAlB_4$ could be examples in this category, although the nature of QCPs in these systems remains to be firmly established.

More recent studies have focused attention, both experimentally and theoretically, on the global phase diagram of antiferromagnetic heavy-fermion metals. Tantalizing evidence has emerged for a non-Fermi liquid phase without any magnetic ordering and with suppressed Kondo entanglement. Whether such a state can in fact arise within the Kondo-lattice model is an intriguing open theoretical question. In the process of addressing such issues, it is becoming clear that quantum fluctuations in heavy-fermion systems can be tuned in more ways than one. Different phases and QCPs may arise when a magnetic disordering is induced by the Kondo coupling between the local moments and conduction electrons or when it is caused by reduced dimensionality and/or magnetic frustration.

Theoretically, an important notion that has emerged from studies in heavy-fermion systems is that quantum criticality can go beyond the Landau paradigm of fluctuations in an order parameter associated with a spontaneous symmetry breaking. This notion has affected the developments on quantum criticality in other systems, including insulating magnets. More generally, quantum criticality in heavy-fermion metals epitomizes the richness and complexity of continuous quantum phase transitions as compared with their classical counterparts. New theoretical methods are needed to study strongly coupled quantum critical systems. One promising new route is provided by an approach that is based on quantum gravity (*49*). Using a charged black hole in a weakly curved space-time to model a finite density of electrons, this approach has provided a tantalizing symmetry reason for some fermionic spectral quantities to display an anomalous frequency dependence when its momentum dependence is smooth. Whether a related symmetry principle underlies the dynamical scaling of the spin response at the Kondo-breakdown local quantum criticality is an intriguing issue for future studies.

The insights gained from these studies on the well-defined QCPs in various heavy-fermion metals have implications for other members of this class of materials as well as for other classes of strongly correlated electronic systems. For example, an outstanding issue is the nature of the hidden-order phase in the heavy-fermion compound URu_2Si_2 (*50*, *51*). This phase is in proximity to some low-temperature magnetically ordered phases, raising the question of the role of quantum phase transitions in this exciting system. In the cuprates, Fermi-surface evolution as a function of doping has also been playing a prominent role in recent years. In light of the discussions on the possible role of doping-induced QCPs, it appears likely that some of the physics discussed for heavy-fermion quantum criticality also comes into play in the cuprates (*52*). For the iron pnictides, the magnetic/superconducting phase diagram has also been observed to show a striking resemblance to Fig. 1A. The interplay between magnetic quantum criticality, electronic localization, and unconventional superconductivity, which has featured so prominently in the systems considered here, is probably pertinent to heavy-fermion metals in general as well as other classes of correlated-electron materials, including the iron pnictides and organic charge-transfer salts. Quantum phase transitions are also being discussed in broader settings, such as ultracold atomic gases and quark matter. It is conceivable that issues related to our discussion here will come into play in those systems as well.

References and Notes

1. I. Osborne, R. Coontz, *Science* **319**, 1201 (2008).
2. Special Issue, *Phys. Status Solidi B* **247**, 457 (2010).
3. F. M. Grosche *et al.*, *J. Phys. Condens. Matter* **13**, 2845 (2001).
4. P. Gegenwart, Q. Si, F. Steglich, *Nat. Phys.* **4**, 186 (2008).
5. Y. Tokiwa, T. Radu, C. Geibel, F. Steglich, P. Gegenwart, *Phys. Rev. Lett.* **102**, 066401 (2009).
6. A. W. Rost, R. S. Perry, J.-F. Mercure, A. P. Mackenzie, S. A. Grigera, *Science* **325**, 1360 (2009).
7. J. Custers *et al.*, *Nature* **424**, 524 (2003).
8. S. Friedemann *et al.*, *Nat. Phys.* **5**, 465 (2009).
9. M. B. Maple *et al.*, *J. Low Temp. Phys.* **95**, 225 (1994).
10. A. C. Hewson, *The Kondo Problem to Heavy Fermions* (Cambridge Univ. Press, Cambridge, 1993).
11. R. A. Cooper *et al.*, *Science* **323**, 603 (2009).
12. S. A. Grigera *et al.*, *Science* **294**, 329 (2001).
13. G. R. Stewart, *Rev. Mod. Phys.* **73**, 797 (2001).
14. H. v. Löhneysen, A. Rosch, M. Vojta, P. Wölfle, *Rev. Mod. Phys.* **79**, 1015 (2007).
15. F. Steglich *et al.*, *Phys. Rev. Lett.* **43**, 1892 (1979).
16. H. Hegger *et al.*, *Phys. Rev. Lett.* **84**, 4986 (2000).
17. Q. Si, S. Rabello, K. Ingersent, J. L. Smith, *Nature* **413**, 804 (2001).
18. P. Coleman, C. Pépin, Q. Si, R. Ramazashvili, *J. Phys. Condens. Matter* **13**, R723 (2001).
19. T. Senthil, M. Vojta, S. Sachdev, *Phys. Rev. B* **69**, 035111 (2004).
20. I. Paul, C. Pépin, M. R. Norman, *Phys. Rev. Lett.* **98**, 026402 (2007).
21. S. Nakatsuji *et al.*, *Nat. Phys.* **4**, 603 (2008).
22. Q. Si, *Physica B* **378**, 23 (2006).
23. S. Doniach, *Physica B* **91**, 231 (1977).
24. C. M. Varma, *Rev. Mod. Phys.* **48**, 219 (1976).
25. S.-K. Ma, *Modern Theory of Critical Phenomena* (Addison-Wesley, Redwood City, CA, 1976).
26. J. A. Hertz, *Phys. Rev. B* **14**, 1165 (1976).
27. C. D. Bredl, F. Steglich, K. D. Schotte, *Z. Phys. B* **29**, 327 (1978).
28. A. J. Millis, *Phys. Rev. B* **48**, 7183 (1993).
29. T. Moriya, *Spin Fluctuations in Itinerant Electron Magnetism* (Springer, Berlin, 1985).
30. M. A. Continentino, *Phys. Rev. B* **47**, 11587 (1993).
31. O. Stockert *et al.*, *Phys. Rev. Lett.* **92**, 136401 (2004).
32. O. Stockert *et al.*, *Physica B* **403**, 973 (2008).
33. W. Knafo, S. Raymond, P. Lejay, J. Flouquet, *Nat. Phys.* **5**, 753 (2009).
34. M. C. Aronson *et al.*, *Phys. Rev. Lett.* **75**, 725 (1995).
35. A. Schröder *et al.*, *Nature* **407**, 351 (2000).
36. H. Shishido, R. Settai, H. Harima, Y. Ōnuki, *J. Phys. Soc. Jpn.* **74**, 1103 (2005).
37. T. Park *et al.*, *Nature* **440**, 65 (2006).
38. S. Watanabe, A. Tsuruta, K. Miyake, J. Flouquet, *J. Phys. Soc. Jpn.* **78**, 104706 (2009).
39. S. Paschen *et al.*, *Nature* **432**, 881 (2004).
40. S. Hartmann *et al.*, *Phys. Rev. Lett.* **104**, 096401 (2009).
41. P. Gegenwart *et al.*, *Science* **315**, 969 (2007).
42. M. Klein *et al.*, *Phys. Rev. Lett.* **101**, 266404 (2008).
43. S. Friedemann *et al.*, *Proc. Natl. Acad. Sci. U.S.A.* (2010).
44. Y. Tokiwa, P. Gegenwart, C. Geibel, F. Steglich, *J. Phys. Soc. Jpn.* **78**, 123708 (2009).
45. L. Balents, *Nature* **464**, 199 (2010).
46. H. Shishido *et al.*, *Science* **327**, 980 (2010).
47. O. Stockert, M. Enderle, H. v. Löhneysen, *Phys. Rev. Lett.* **99**, 237203 (2007).
48. S. E. Sebastian *et al.*, *Proc. Natl. Acad. Sci. U.S.A.* **106**, 7741 (2009).
49. I. R. Klebanov, J. M. Maldacena, *Phys. Today* **62**, 28 (2009).
50. A. R. Schmidt *et al.*, *Nature* **465**, 570 (2010).
51. P. Aynajian *et al.*, *Proc. Natl. Acad. Sci. U.S.A.* **107**, 10383 (2010).
52. N. Doiron-Leyraud *et al.*, *Nature* **447**, 565 (2007).

53. We thank E. Abrahams, M. Brando, P. Coleman, S. Friedemann, P. Gegenwart, C. Geibel, F. M. Grosche, S. Kirchner, C. Krellner, M. Nicklas, T. Park, J. Pixley, O. Stockert, J. D. Thompson, S. Wirth, and S. Yamamoto for useful discussions. This work has been supported by NSF and the Robert A. Welch Foundation grant C-1411 (Q.S.) and by the DFG Research Unit 960 "Quantum Phase Transitions" (F.S.).

10.1126/science.1191195

Science

Heavy Fermions and Quantum Phase Transitions

Qimiao Si and Frank Steglich

Science **329** (5996), 1161-1166.
DOI: 10.1126/science.1191195

From Simplicity to Complexity
The relatively simple properties of isolated electrons become rich and complex when the particle-particle interactions are strong enough to form a correlated system. Emergence of complex behavior from relatively simple subunits is an intensely studied topic in condensed-matter physics and applies to many systems in superconductivity and magnetism. **Si and Steglich** (p. 1161) review the physics of heavy fermion intermetallic compounds. These make ideal materials for study because they can exhibit metallic, magnetic, and superconducting behavior showing novel quantum phases and unconventional quantum criticality.